processes

MDPI

Article

Kinetics of Alkyl Lactate Formation from the Alcoholysis of Poly(Lactic Acid)

Fabio M. Lamberti [1], Luis A. Román-Ramírez [1], Paul Mckeown [2], Matthew D. Jones [2] and Joseph Wood [1,*]

[1] School of Chemical Engineering, University of Birmingham, Edgbaston, Birmingham B15 2TT, UK; fxl876@student.bham.ac.uk (F.M.L.); larbham@gmail.com (L.A.R.-R.)

[2] Department of Chemistry, University of Bath, Claverton Down, Bath BA2 7AY, UK; pm482@bath.ac.uk (P.M.); mj205@bath.ac.uk (M.D.J.)

* Correspondence: J.Wood@bham.ac.uk

Received: 8 June 2020; Accepted: 23 June 2020; Published: 24 June 2020

Abstract: Alkyl lactates are green solvents that are successfully employed in several industries such as pharmaceutical, food and agricultural. They are considered prospective renewable substitutes for petroleum-derived solvents and the opportunity exists to obtain these valuable chemicals from the chemical recycling of waste poly(lactic acid). Alkyl lactates (ethyl lactate, propyl lactate and butyl lactate) were obtained from the catalysed alcoholysis reaction of poly(lactic acid) with the corresponding linear alcohol. Reactions were catalysed by a Zn complex synthesised from an ethylenediamine Schiff base. The reactions were studied in the 50–130 °C range depending on the alcohol, at autogenous pressure. Arrhenius temperature-dependent parameters (activation energies and pre-exponential factors) were estimated for the formation of the lactates. The activation energies (Ea_1, Ea_2 and Ea_{-2}) for alcoholysis in ethanol were 62.58, 55.61 and 54.11 kJ/mol, respectively. Alcoholysis proceeded fastest in ethanol in comparison to propanol and butanol and reasonable rates can be achieved in temperatures as low as 50 °C. This is a promising reaction that could be used to recycle end-of-life poly(lactic acid) and could help create a circular production economy.

Keywords: Alkyl lactate; alcoholysis; poly(lactic acid), chemical recycling; kinetics

1. Introduction

Alkyl lactates (AL) are classified as green solvents according to the principles of green chemistry, and are considered prospective renewable substitutes for petroleum-derived solvents [1–3]. ALs do not present potential health risks in terms of teratogenicity, maternal toxicity or systemic toxicity [4]. Biodegradability and ecotoxicological studies have also shown that they are environmental-friendly compounds with low ecotoxicity [5,6].

ALs are already employed in several industries such as the pharmaceutical, food, agricultural and polymer industries and their use is expected to increase further in the near future [1,7]. The market value of ethyl lactate (EtLa) alone is estimated to reach USD 92 million by 2024 [8]. EtLa is an additive in paints, foods, cosmetics and cleaning items, as well as a solvent in the manufacturing of microelectronics and pharmaceutical products [7,9,10]. Studies have also shown the possibility of using EtLa for the recovery of phenolics and carotenoids (phytonutrients) from fruits and vegetables including palm oil [11–13]. More recently, Planer, et al. [14] have demonstrated the use of EtLa as a solvent in olefin metathesis. Its application as an entrainer in the reactive distillation of azeotropic mixtures of methyl acetate and methanol has also been exhibited [15].

Similarly, propyl lactate (PrLa) is a pesticide and a food additive, whereas *n*-butyl lactate (BuLa) is an additive and a solvent in food, pharmaceuticals, cosmetics and paint formulations [9,16,17]. The

use of BuLa lactate in the recovery of bio-butanol from aqueous mixtures has also been reported [18]. Additionally, ALs are building blocks of valuable chemicals. Propylene glycol, a main chemical for polymer production, can be synthesised from lactic acid and its esters [19,20]. Likewise, diynones, a group of starting materials for a range of chemicals, can be produced from EtLa [21].

Production routes of ALs include hydroformylation of vinyl acetate, carbonylation of acetaldehyde, hydrogenation of pyruvates and the esterification of lactic acid with an alcohol with homogeneous and heterogeneous catalysts, including acid ion-exchange resins [19,22–24]. ALs can also be synthesised from lactide, the dimer of lactic acid, as demonstrated by Bykowski, et al. [23] and Grala, et al. [25]. The catalytic synthesis from biomass has been reviewed by Mäki-Arvela, et al. [26]. High EtLa selectivities (>95%) from the reaction of dihydroxyacetone and ethanol (EtOH) catalysed by methyl-functionalised tin silicates has been demonstrated [27]. High AL yields (around 96%) were also obtained by using protic ionic liquids formulated from a nitrogen base and sulphuric acid by Dorosz, et al. [9].

ALs can also be produced from the alcoholysis reaction of poly(lactic acid) (PLA) [28–34]. PLA is seen as a substitute for petroleum-derived polymers that can be produced from renewable sources [35]. Although PLA can be degraded under controlled conditions (composting) its long degradability in natural conditions can contribute to plastic pollution [34,36,37]. Therefore, suitable controlled degradation methods such as alcoholysis are an alternative to treat end-of-life PLA. Significantly, a circular economy system is possible when lactide, the dimer of lactic acid used in the ring opening polymerization (ROP) of PLA, is synthesised from alkyl lactates [38–42]. With a circular economy in mind, Jones and co-workers have also developed a series of Zn-based complex catalysts suitable for both, the ROP of lactide and for the depolymerisation of PLA [33,34,43–45].

The impact of different recycling methods for PLA has been investigated in literature. Life cycle assessment (LCA) comparing PLA disposal methods such as composting and mechanical and chemical recycling found that mechanical recycling has the lowest environment impact in terms of climate change, human toxicity and fossil depletion [28]. The next lowest LCA impact is chemical recycling, after which is composting. Although mechanical recycling has the smallest LCA impact it leads to a buildup of impurities and reduced mechanical properties of the recycled PLA. The impact of recycling PLA on other waste streams has also been investigated in literature. PLA has been shown to have a severe incompatibility with PET recycling [46]. PLA content as low as 1000 ppm causes noticeable hazing and degradation of the recycled PET and the low melting temperature (T_m) of PLA (155 °C) results in serious disruption during melt reprocessing of PET [47].

In this work, the EtLa, PrLa and BuLa were produced from the catalysed alcoholysis of PLA with the corresponding alcohol. PLA alcoholysis is in principle a transesterification reaction; which involves an alcohol nucleophile attacking the ester linkages along the PLA backbone. The methine protons were considered to be in one of three different environments—internal methine (Int), chain-end (CE) or alkyl lactate (AL). The relative concentrations of the methines were calculated from NMR spectra. A fully-characterized Zn complex used in the polymerisation of lactide was employed in this work for the depolymerisation process [34]. Selectivities and yields of green solvent as a function of temperature and chain length are presented as well as kinetic parameters of the reactions.

2. Materials & Methods

2.1. Materials

PLA pellets, supplied by NatureWorks (Ingeo™ 6202D) were used without pre-treatment. All reactants were HPLC grade: ethanol (EtOH, ≥99.8%), propan-1-ol (PrOH, ≥99% and butan-1-ol (BuOH, ≥99%) were purchased from Fisher scientific. Tetrahydrofuran (THF, HPLC grade, ≥99.9% without inhibitor) was purchased from Honeywell. All chemicals were used as received. Helium CP grade (≥99.999% purity), nitrogen (oxygen-free, ≥99.998%) and argon (≥99.998%) were purchased from BOC.

2.2. Catalyst Preparation

Zinc ethylenediamine Schiff-based complex, Zn(**1**)$_2$, and propylenediamine Schiff-based complex, Zn(**2**)$_2$, were prepared and isolated as one pure species according to literature methods, with structure shown in (Figure 1) [33,34,48]. Preparation was carried out on a multi-gram scale (<25 g) and the catalysts stored under inert conditions prior to use. Purity was confirmed via NMR spectroscopy and elemental analysis. It was previously shown that Zn(**1**)$_2$ remains intact after reaction, whereas, Zn(**2**)$_2$ forms a new species under reaction conditions [33,48].

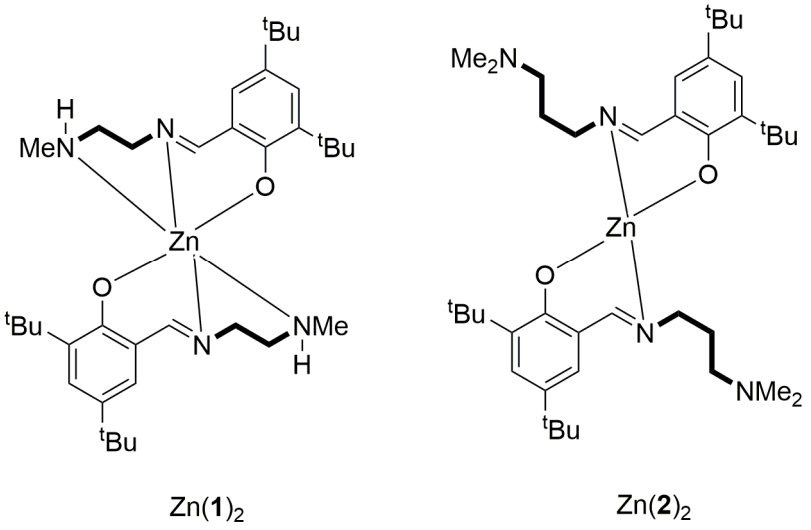

Figure 1. Chemical structure of the two catalysts zinc ethylenediamine Schiff-based complex (Zn(**1**)$_2$) and propylenediamine Schiff-based complex (Zn(**2**)$_2$).

2.3. Apparatus and Procedure

After the successful demonstration of the catalyst on small-scale experiments, further scale-up tests were undertaken and are reported in this paper. The experiments were carried out in a 300 mL stirred autoclave (PARR model4566). The temperature inside the reactor was controlled by an oil bath heating circulator (IKA CBC5-Control) connected to the reactor's jacket.

In each experiment, 12.5 g of PLA, 250 mL of THF and 1 g of Zn(**1**)$_2$ (8 wt.%) were charged to the reactor. The autoclave was then sealed and degassed with N_2 for at least 20 min before bringing the reactor to the desired working temperature (50–130 °C) at stirring speed of 300 rpm. The reactor was left at the desired temperature for a further 20 min to ensure all the PLA pellets were dissolved then 50 mL of alcohol (either EtOH, PrOH or BuOH) was fed into the reactor via an HPLC pump at a rate of 10 mL/min. Samples were taken periodically and tested by GC and sent for further ^{1}H NMR analysis. The product yields are based on the NMR data. The employed protocol was identical for Zn(**2**)$_2$ experiments except the stirring speed was 800 rpm as Zn(**2**)$_2$ showed mass transport limitations at 300 rpm. It was previously demonstrated with MeOH and EtOH at the same concentration and reaction parameters that the identity of the alcohol has a pronounced impact on reaction rate [33]. In this study we sought to use different alcohols at a fixed reaction volume. In any case, the amount of alcohol is still in excess relative to the PLA ester groups.

2.4. GC and NMR

Alkyl lactate concentration was assessed by a gas chromatograph (GC) coupled with Flame-Ionization Detection (FID) (Agilent Technologies, 6890N). Samples were injected by an autosampler (Agilent Technologies, 7683B), to a 30 m × 0.32 mm ID, 0.25 μm film thickness HP-5 Agilent capillary column using helium as carrier and make-up gas with the following conditions: inlet temperature of 150 °C, 1 μL injection volume, 1:400 split ratio, 250 °C detector temperature, with an initial oven temperature of 65 °C (held for 4 min), then 100 °C min^{-1} ramp to 195 °C (held for 1 min), followed by

100 °C min^{-1} ramp to 230 °C (held for 5 min). Initial flowrate was 0.8 mL min^{-1} (held for 5 min), then 100 mL min^{-1} ramp to 3 mL min^{-1} (held for 5 min). A multiple point external standard calibration curve was prepared using standard solutions covering the range of alkyl lactate concentration. A linear response of the detector was determined for EtLa and BuLa (R^2 = 0.9997 and 0.9996, respectively). For PrLa the GC analysis was only qualitative.

^{1}H NMR spectra were measured using a 400 MHz Bruker Avance II spectrometer. Samples were dissolved in, and referenced to, C_6D_6. A virtual concentration of methine functional groups was measured as a relative percentage. The methine protons were considered to be in one of three different environments—alkyl lactate (AL) (4.23–4.29 ppm), chain-end (CE) (4.30–4.39 ppm/5.09–5.21 ppm) or internal (Int) (5.09–5.21 ppm).

2.5. Kinetic Modelling

The experimental data were modelled using the reaction mechanism proposed by Román-Ramírez, et al. [34], in which AL is formed through a consecutive reaction where PLA internal methine groups (Int) degrade in a first step into chain-end methine groups (CE) and then through a reversible reaction the CE converts into AL (Equation (1)). For clarity, the set of differential equations resulting from the mass balance on the batch reactor is presented here in Equations (2)–(4).

$$Int \overset{k_1}{\rightarrow} CE \underset{k_{-2}}{\overset{k_2}{\rightleftarrows}} AL \quad (1)$$

$$\frac{dInt}{dt} = -k_1 Int \quad (2)$$

$$\frac{dCE}{dt} = k_1 Int - k_2 CE + k_{-2} AL \quad (3)$$

$$\frac{dAL}{dt} = k_2 CE - k_{-2} AL \quad (4)$$

3. Results

3.1. NMR Results

Table 1 shows the results of PLA alcoholysis using various alcohols over a range of temperatures (50–130 °C). AL yield (%) was calculated from NMR data. The working hypothesis was that longer-chain alcohols would sterically hinder the PLA alcoholysis reaction. Initial reaction rates were calculated as the initial rate of AL formation at 120 min. The times taken to reach 61% AL are shown for the purpose of comparing the time required for the same-extent reaction for the different alcohols and conditions. Also shown in Table 1 are the results from experiments using Zn(**2**)$_2$; this catalyst outperformed Zn(**1**)$_2$ at 50 °C with higher reaction rates but had less competitive rates at all other temperatures.

Table 1. Time taken to reach high AL yield for different alcohols at different temperatures.

Alcohol	Temperature (°C)	Alky Lactate Yield (%)	Final Time (min)	Time Taken to Reach 61% AL (min)	Initial Reaction Rate ($g \cdot mL^{-1} \cdot min^{-1}$)
EtOH	50	81	4650	2748	6.66×10^{-6}
EtOH[a]	50	86	1350	110	4.13×10^{-4}
EtOH	70	91	1920	775	6×10^{-5}
EtOH[a]	70	79	8700	5452	7.33×10^{-5}
EtOH	90	93	540	195	2.8×10^{-4}
EtOH[a]	90	83	38 70	1840	5.33×10^{-5}
EtOH	110	96	420	108	4.53×10^{-4}
EtOH[a]	110	96	1440	504	1.13×10^{-4}
PrOH[a]	50	72	1509	194	4.35×10^{-4}
PrOH	90	92	2796	828	8.25×10^{-5}
PrOH	110	91	1260	343	2.1×10^{-4}
PrOH[a]	110	61	1428	1428	3.75×10^{-5}
PrOH	130	92	590	207	3×10^{-4}
BuOH	90	78	7548	2647	5.8×10^{-5}
BuOH	110	88	1143	369	2.56×10^{-4}
BuOH[a]	110	75	1986	1286	3.3×10^{-5}
BuOH	130	89	600	225	3.3×10^{-4}

[a] = Zn(**2**)$_2$ was used instead of Zn(**1**)$_2$. Where superscript not shown Zn(**1**)$_2$ was used.

Comparing the results of both catalysts, alcoholysis in EtOH at 50 °C using Zn(**2**)$_2$ achieved a higher yield of AL (86% at 1350 min), which was only a fraction of the time taken when using Zn(**1**)$_2$ (81% at 4650 min). At temperatures higher than 50 °C, Zn(**2**)$_2$ did not perform as well as Zn(**1**)$_2$. Looking at EtOH alcoholysis at 70 °C, Zn(**1**)$_2$ achieved an AL yield of 91% in 1920 min, whereas, the less competitive Zn(**2**)$_2$ only achieved an AL yield of 79% in 8700 min. At 90 °C EtOH alcoholysis using Zn(**1**)$_2$ generated an AL yield of 93% in 540 min, but again Zn(**2**)$_2$ was less competitive achieving an AL yield of only 83% in 3870 min. The same pattern was seen when looking at the 110 °C EtOH experiments; Zn(**1**)$_2$ produced an AL yield of 96% in just 420 min whereas, Zn(**2**)$_2$ produced an AL yield of 96% in 1440 min. It is evident that Zn(**2**)$_2$ is the superior catalyst at 50 °C while Zn(**1**)$_2$ is the superior catalyst at higher temperatures. The same pattern appears in experiments with PrOH and BuOH as the alcohol substrates. At 110 °C alcoholysis in PrOH using Zn(**1**)$_2$ generated the higher AL yield of 91% in 1260 min while, Zn(**2**)$_2$ only produced an AL yield of 61% in 1428 min. At 110 °C alcoholysis in BuOH using Zn(**1**)$_2$ generated the higher AL yield of 88% in 1143 min, while the less-competitive Zn(**2**)$_2$ produced an AL yield of 75% in 1986 min. Zn(**1**)$_2$ alcoholysis experiments at 50 °C and 70 °C in PrOH and BuOH were attempted and abandoned for being too slow, however, Zn(**2**)$_2$ was used in PrOH at 50 °C and generated a reasonable yield of AL 72% in only 1509 min.

The EtOH alcoholysis experiments in comparison to PrOH and BuOH achieved higher yields (>90%) of AL in much shorter times; at 90 °C alcoholysis in EtOH achieved an AL yield of 93% in 540 min, whereas, PrOH and BuOH at the same temperature achieved yields of 92% and 78% in 2796 min and 7548 min, respectively. The difference in the reaction rates could be attributed to the increased steric hinderance of the longer-chain alcohols. Comparing all three alcohols at 110 °C; EtOH achieved AL yield of 96% in 420 min and PrOH achieved AL yield of 91% in 1260 min, whereas BuOH achieved AL yield of 88% in 1143 min. Again, the shorter-chain alcohol EtOH outperformed the other two under the same reaction conditions. It is interesting to note that although PrOH had a higher initial reaction rate than BuOH at 90 °C (8.25×10^{-5} $g \cdot mL^{-1} \cdot min^{-1}$ vs. 5.8×10^{-5} $g \cdot mL^{-1} \cdot min^{-1}$) at 110 °C and 130 °C, BuOH had the higher rate although they are very similar.

The different reaction rates could be perhaps be explained by the different boiling points (PrOH T_b = 97 °C, BuOH T_b = 117.7 °C). The reaction temperature of 90 °C was below both alcohols' boiling points therefore the only difference was the additional steric hinderance of BuOH, which is why it had a slower initial reaction rate. At 110 °C PrOH had evaporated while BuOH had not. This could

mean there were fewer PrOH molecules available for reaction which could explain while BuOH has the higher reaction rate of 2.56×10^{-4} g·mL^{-1}·min^{-1} (vs. 2.1×10^{-4} g·mL^{-1}·min^{-1}). At 130 °C both alcohols have evaporated; BuOH still has the higher rate of 3.3×10^{-4} g·mL^{-1}·min^{-1} vs. 3×10^{-4} g·mL^{-1}·min^{-1} for PrOH, but the difference between these rates was smaller than the difference between the rates at 110 °C. After plotting the concentration of the AL for each alcoholysis reaction at 90 °C it could clearly be seen that higher concentrations of AL were achieved much faster for EtOH, then PrOH and finally BuOH (Figure 2).

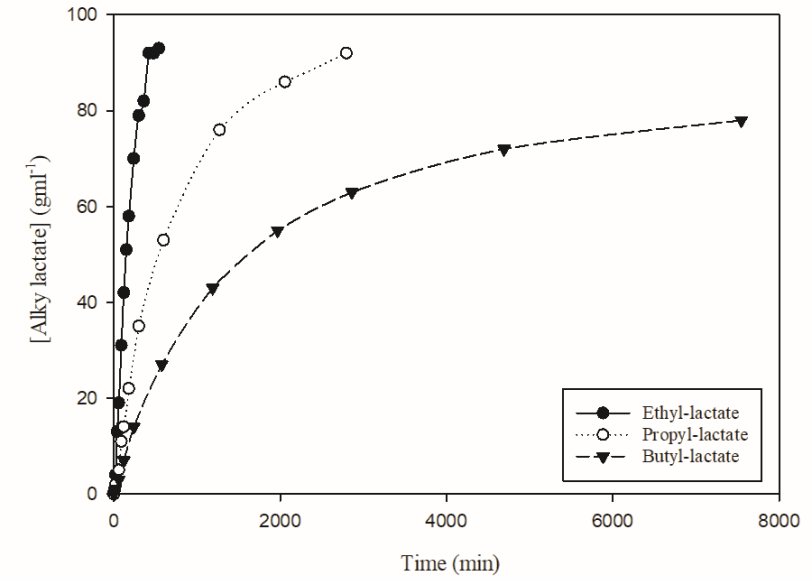

Figure 2. Alky-lactate concentration vs. time for Zn(**1**)$_2$ experiments at 90 °C (based on GC and NMR data).

3.2. Arrhenius Temperature-Dependent Parameters

Relative concentrations of Int, CE and AL methine groups were generated from NMR data of each experiment. The relative concentrations were fitted to the kinetic model proposed by Román-Ramírez, et al. [34] described in Equation (1), the resulting rate equations were solved numerically in Matlab in order to fit the model to the experimental data and thus estimate the rate coefficients for the different experimental conditions (Table 2). Two typical reactions profiles are shown for EtLa and BuLa at 110 °C catalysed by Zn(**1**)$_2$ (Figure 3). Figure 3 reaction profile A shows ethanol alcoholysis of PLA; the experimental data fits the model nicely. Reaction profile B shows butanol alcoholysis; the experimental data deviates from the model slightly.

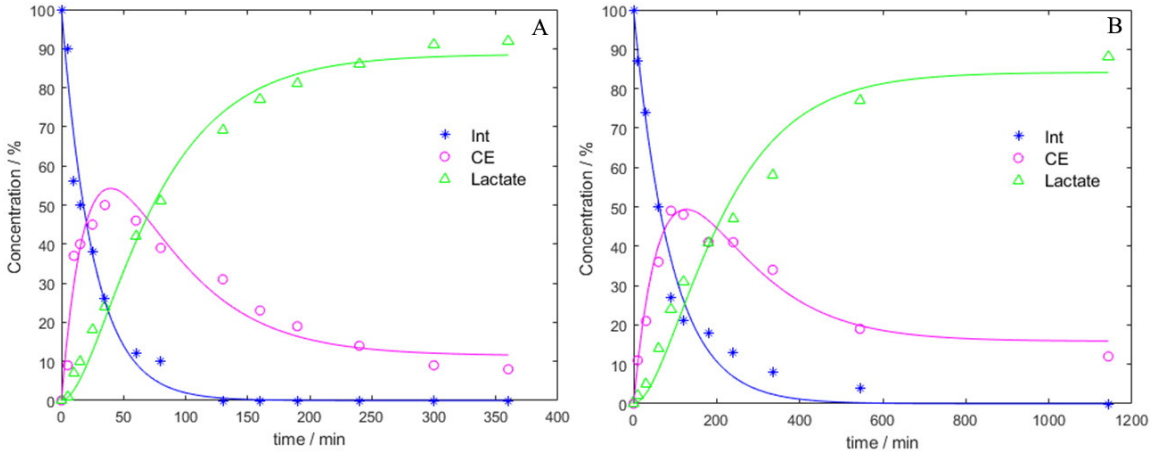

Figure 3. Reaction profiles obtained from NMR data for alcoholysis at 110 °C with Zn(**1**)$_2$. (**A)** EtLa and (**B)** BuLa.

Table 2. Rate coefficients for each experiment catalysed by Zn(**1**)$_2$.

Alcohol	Temp (°C)	k_1 (min^{-1})	k_2 (min^{-1})	k_{-2} (min^{-1})
EtOH	110	0.0392 ± 0.0034	0.0163 ± 0.0021	0.0021 ± 0.0009
EtOH	90	0.0171 ± 0.0008	0.0087 ± 0.0005	0.0007 ± 0.0002
EtOH	70	0.0051 ± 0.0004	0.0023 ± 0.0003	0.0003 ± 0.0002
EtOH	50	0.0010 ± 0.0006	0.0007 ± 0.0008	0.0001 ± 0.0006
PrOH	130	0.0197 ± 0.0010	0.0081 ± 0.0006	0.0009 ± 0.0004
PrOH	110	0.0139 ± 0.0009	0.0049 ± 0.0005	0.0007 ± 0.0003
PrOH	90	0.0062 ± 0.0006	0.0028 ± 0.0005	0.0005 ± 0.0002
BuOH	130	0.0170 ± 0.0010	0.0072 ± 0.0006	0.0010 ± 0.0004
BuOH	110	0.0111 ± 0.0010	0.0061 ± 0.0010	0.0012 ± 0.0006
BuOH	90	0.0031 ± 0.0005	0.0011 ± 0.0003	0.0004 ± 0.0002

The rate coefficients from Table 2 were used to generate Arrhenius plots for each of the alcoholysis reactions. According to Equation (1), alcoholysis of PLA occurs in three steps, therefore, there are three sets of rate coefficients (k_1, k_2 and k_{-2}) which correspond to three different activation energies (Ea_1, Ea_2 and Ea_{-2}). The activation energies for each individual step were obtained from the gradient of the Arrhenius plots (Figure 4).

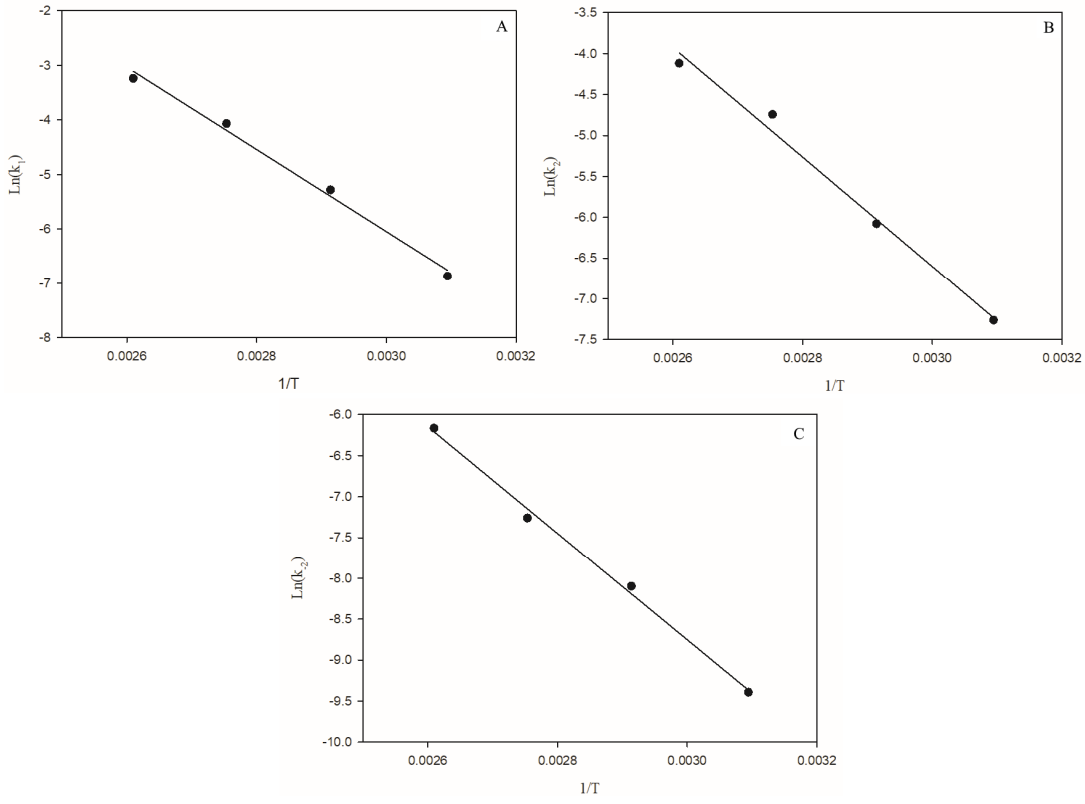

Figure 4. Arrhenius plots for EtOH experiments at 50–110 °C, line of best fit of the rate coefficients. (**A)** k_1 rate coefficient, (**B)** k_2 rate coefficient and (**C)** k_{-2} rate coefficient.

Table 3 shows the activation energies of each of the individual steps of PLA alcoholysis in EtOH. Unfortunately, because only three temperature ranges were obtained for PrOH and BuOH the confidence interval for their resulting Arrhenius plots was considered too great to be reliable so their resulting activation energies were too unreliable to use. Therefore, Table 3 only includes activation energies for EtOH alcoholysis and, as a comparison, the activation energies for MeOH from a previous paper from the same research group [34].

Table 3. The activation energies for each step of PLA alcoholysis to produce AL.

Alcoholysis	Ea_1 (kJ/mol)	Ea_2 (kJ/mol)	Ea_{-2} (kJ/mol)
MeOH	40.8 ± 2.3	44.7 ± 2.8	40.8 ± 21.1
EtOH	62.58 ± 16.94	55.61 ± 17.72	54.11 ± 10.92

According to Table 3 all three activation energies for EtOH were higher than those for MeOH, although only Ea_1 was higher than MeOH within its confidence intervals. EtOH alcoholysis displaying higher activation energies is in agreement with the working hypothesis, namely longer chain alcohols will sterically hinder the PLA alcoholysis reaction. Additionally, because of its small size MeOH is considered a stronger nucleophile so can approach the polymer chain more easily before donating its lone pair of electrons. The smaller size of MeOH means it more easily penetrates the amorphous regions of PLA, increasing the likelihood of ester bond cleavages.

4. Discussion

According to Equation (1), the first step of the reaction, represented by the coefficient k_1, is the initial cleavage of the PLA chain—the alcohol nucleophile randomly attacks any of the ester linkages along the PLA chain. A transesterification reaction occurs which generates two CE groups for each Int ester cleavage. The relative concentration of the Int groups decreases with reaction time and the concentration of the CE groups increases. Multiple chain scission reactions occur where the alcohol nucleophile attacks and cleaves the Int ester linkages of oligomer fragments that also contain CE groups (Figure 5). The second step of the reaction is an equilibrium process represented by the coefficients (k_2/k_{-2}). The forward step, represented by k_2, occurs when the alcohol nucleophile attacks an ester linkage adjacent to a CE group, forming the value-added product AL. It is important to note the backwards reaction represented by k_{-2} involves the alcohol group of the AL acting as the nucleophile, attacking the ester carbonyl of the CE oligomers to form a larger oligomer. Since the rate of reaction is determined by AL product formation, increase in the rate of the reverse step k_{-2}, will lead to decrease in the overall rate of reaction.

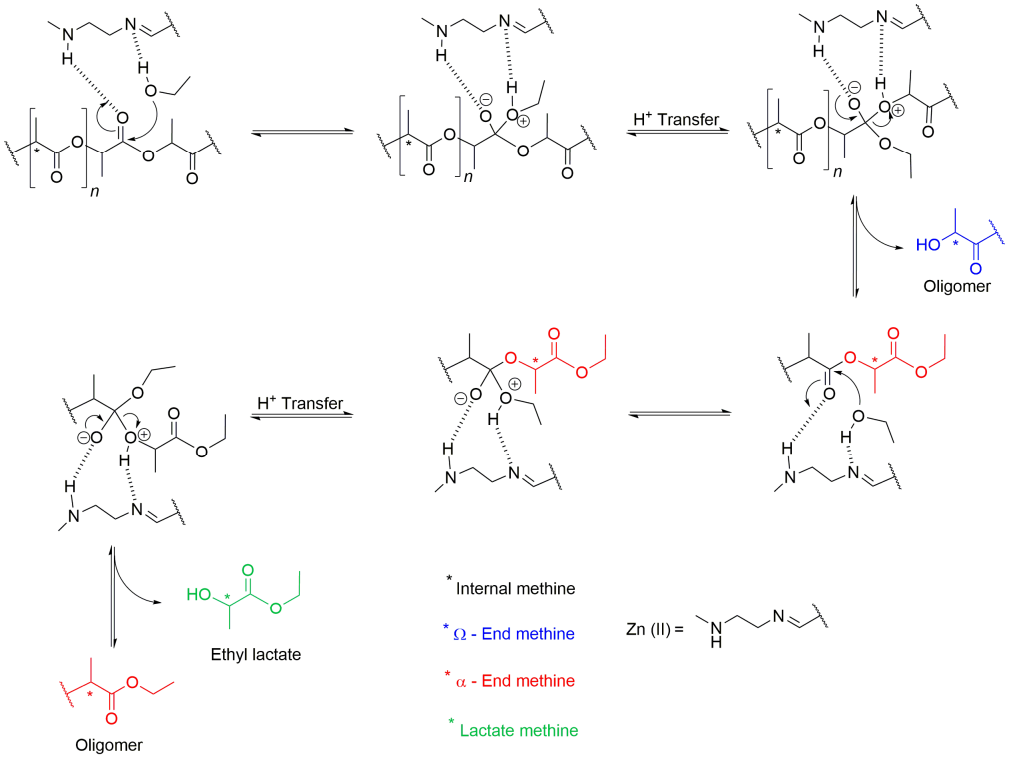

Figure 5. Proposed mechanism for transesterification reaction of PLA using ethanol and Zn (**1**)$_2$.

The working hypothesis predicted that increasing the chain length of the alcohol would result in a slower reaction rate and AL product formation. This is based on the assumption that the nucleophilic ability decreases from MeOH to BuOH in the polar aprotic solvent THF due to increased steric hinderance; since the transesterification reaction mechanism requires the catalyst to coordinate to both the PLA chain and the alcohol, the larger alcohol groups will be more sterically hindered. The data from Table 1 shows that EtOH alcoholysis produced a higher concentration of AL in the shortest time compared to PrOH and the slowest, BuOH. The data from Table 3 shows EtOH alcoholysis had a higher activation energy for Int ester cleavage than MeOH alcoholysis (Figure 6). Both of these results support the working hypothesis that a longer carbon chain alcohol would sterically hinder the formation of the zinc alcohol–PLA ester coordination complex, which is a necessary transition state for the reaction to take place.

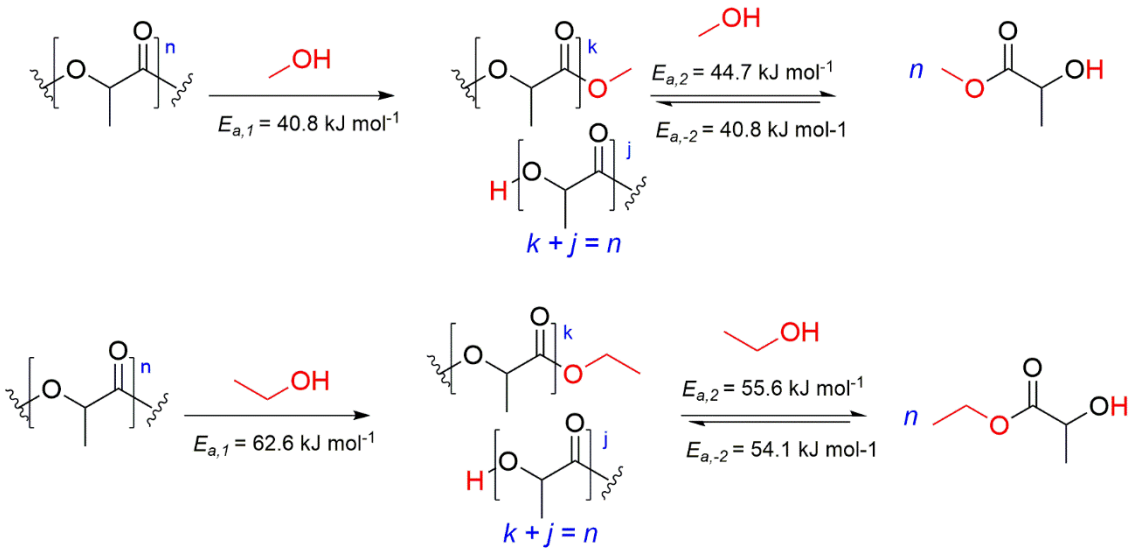

Figure 6. Simplified reaction scheme for PLA alcoholysis showing the activation energies for each step.

These experiments only investigated one molecular weight of PLA pellet (Ingeo™ 6202D). Previous work [34] looked at alcoholysis of PLA pellets in MeOH and investigated a range of different PLA molecular weights. Although the researchers reduced the size of the PLA pellets to assist dissolution, they concluded that the rate of degradation was independent of polymer molecular weight. If larger pellets of PLA are used then dissolution will take longer, but, since the reactions were only started with addition of the alcohol after complete dissolution of PLA, larger sizes or different molecular weights should not affect the kinetics.

Previous work [45] showed that Zn(**2**)$_2$ has non-Arrhenius behaviour and works well at low temperature; these small scale reactions worked well and produced reasonable results while remaining reproducible. This was the reasoning for attempting to scale up Zn(**2**)$_2$ alcoholysis in this paper, although the catalyst worked very well at 50 °C the results were subject to reproducibility issues. It was concluded that Zn(**2**)$_2$ is a more sensitive catalyst than Zn(**1**)$_2$ as the alcohol chain length increases and that there were also some unknown variables in the procedure that would interact with the catalyst and decrease its activity. If the stability of Zn(**2**)$_2$ could be improved then this catalyst would have a huge potential in industrial reactions, due to its remarkably fast kinetics at such a low temperatures and hence low operating cost.

Similar to previous observations for MeOH [45], Zn(**2**)$_2$ exhibited a very interesting property; AL formation was observed even at sub-zero temperatures. When Zn(**2**)$_2$ was used in 50 °C experiments and after ending the reaction the samples were placed in the freezer with temperatures below 0 °C. After a few days the samples were re-analysed via GC and NMR and it was found that the relative concentration of Int had decreased, while the concentrations of CE and AL had increased,

thus implying that the reaction had continued even at conditions below 0 °C. This phenomenon was still present when experiment samples previously reacted at higher temperatures were placed in the freezer, however, the increase in concentration of CE and AL was significantly less than that seen in lower-temperature experiments. An example of this was when two samples with similar composition of Int, CE and AL, such as a samples taken after 5 min reaction time from an experiment conducted at 50 °C and an experiment conducted at 110 °C, were both placed in the freezer for a few days. After this time, they were reanalysed and the 110 °C sample had only a small increase in CE and AL, whereas, the 50 °C sample had almost no Int and a very high increase in CE and AL. Furthermore, the phenomenon was most evident with EtOH experiments then to a lesser extent in PrOH and least in BuOH. As suggested in [45] the non-Arrhenius behaviour is attributed to the formation of a catalyst–complex intermediate, . This intermediate shows collision stability as higher stirring speeds increase reaction rates. The sub-zero temperatures could help stabilise the catalyst–complex intermediate, moreover, the phenomenon was seen to a lesser effect for longer-chain alcohols which could suggest that the longer chain sterically hinders the formation of the intermediate complex.

Using EtOH as the nucleophile for PLA alcoholysis shows that relatively quick rates can be achieved at temperatures as low at 50 °C, the low temperature requirement potentially leading to lower operating costs if the process were to be operated commercially. There is therefore a strong potential to use EtOH for industrial chemical recycling of PLA waste to recover the commercially-valuable EtLa. Out of the three product lactates EtLa, PrLa and BuLa, the former is considered the most useful and has the highest demand [9,10]. EtLa is biodegradable so will eventually degrade and assimilate into plants that can be used as carbohydrate feedstocks to generate virgin PLA [10]. It is also possible to convert EtLa to lactide which can then be repolymerised to PLA. This opens up opportunities to create a truly circular production economy [41].

5. Conclusions

Zn(**1**)$_2$ a catalyst that has previously be shown to be active for the production of methyl lactate from the alcoholysis of PLA, has in this paper been shown to generate EtLa, PrLa and BuLa under the same alcoholysis reaction with the corresponding linear alcohol. This route provides an excellent opportunity to chemically recycle of end-of-life PLA to obtain a value-added product. Of the three ALs investigated, the green solvent EtLa has the highest demand and most commercial value due to its relatively high boiling point, low toxicity and its biodegradability. Additionally, this paper showed that alcoholysis of PLA under EtOH proceeds significantly faster than under either PrOH or BuOH, and under EtOH, it can achieve reasonable rates at temperatures as low as 50 °C. The EtOH alcoholysis reaction would be well suited for an industrial scale-up as such low temperatures would have reasonably low operating costs. Moreover, a continuous type reaction could easily be designed, and product separation could simply be achieved via distillation. Zn(**2**)$_2$ was also investigated and showed non-linear Arrhenius behaviour, working particularly well in the low temperature regime. In fact, at 50 °C Zn(**2**)$_2$ outperformed Zn(**1**)$_2$ and achieved a higher conversion of AL in a fraction of the time. Unfortunately, Zn(**2**)$_2$ has stability issues and is a less-reproducible catalyst but if these limitations were overcome then it would be even more suited to industrial scale-up and alcoholysis of PLA could be achieved relatively quickly with a low operating cost.

Author Contributions: Conceptualization, M.D.J., J.W. and L.A.R.-R.; methodology, L.A.R.-R. and F.M.L.; validation, L.A.R.-R, P.M. and F.M.L.; formal analysis, L.A.R.-R, P.M. and F.M.L.; investigation, F.M.L.; resources, L.A.R.-R, P.M. and F.M.L.; writing—original draft preparation, L.A.R.-R and F.M.L.; writing—review and editing, J.W., P.M., L.A.R.-R and F.M.L.; visualization, F.M.L., P.M. and L.A.R.-R; supervision, J.W. and L.A.R.-R; project administration, M.D.J. and J.W.; funding acquisition, M.D.J. and J.W. All authors have read and agreed to the published version of the manuscript.

Funding: This research was funded by ESPRC, grant number EP/P016405/1 and the APC was funded by the Institutional Open Access Block Grant at the University of Birmingham.

Acknowledgments: NatureWorks LLC are acknowledge for their donation of PLA samples.

Conflicts of Interest: The authors declare no conflict of interest.

Data: Data associated with this paper are available free of charge via edata.bham.ac.uk

References

1. Calvo-Flores, F.G.; Monteagudo-Arrebola, M.J.; Dobado, J.A.; Isac-García, J. Green and Bio-Based Solvents. *Top. Curr. Chem.* **2018**, *376*, 1–40, doi:10.1007/s41061-018-0191-6.
2. Warner, J.C.; Cannon, A.S.; Dye, K.M. Green chemistry. *Environ. Impact Assess. Rev.* **2004**, *24*, 775–799, doi:10.1016/j.eiar.2004.06.006.
3. Jessop, P.G. Searching for green solvents. *Green Chem.* **2011**, *13*, 1391–1398, doi:10.1039/c0gc00797h.
4. Clary, J.J.; Feron, V.J.; Van Velthuijsen, J.A. Safety assessment of lactate esters. *Regul. Toxicol. Pharmacol.* **1998**, *27*, 88–97, doi:10.1006/rtph.1997.1175.
5. Bowmer, C.T.; Hooftman, R.N.; Hanstveit, A.O.; Venderbosch, P.W.M.; Van Der Hoeven, N. The ecotoxicity and the biodegradability of lactic acid, alkyl lactate esters and lactate salts. *Chemosphere* **1998**, *37*, 1317–1333, doi:10.1016/S0045-6535(98)00116-7.
6. Zuriaga, E.; Giner, B.; Ribate, M.P.; García, C.B.; Lomba, L. Exploring the usefulness of key green physicochemical properties: Quantitative structure–activity relationship for solvents from biomass. *Environ. Toxicol. Chem.* **2018**, *37*, 1014–1023, doi:10.1002/etc.4058.
7. Biddy, M.J.; Scarlata, C.J.; Kinchin, C.M. Chemicals from biomass: A market assessment of bioproducts with near-term potential. *NREL Rep.* **2016**, doi:10.2172/1244312.
8. 360 Market Updates Global Ethyl Lactate Market 2019 by Manufacturers, Regions, Type and Application, Forecast to 2024. Available online: https://www.360marketupdates.com/global-ethyl-lactate-market-13806819 (accessed on 21 May 2020)
9. Dorosz, U.; Barteczko, N.; Latos, P.; Erfurt, K.; Pankalla, E.; Chrobok, A. Highly efficient biphasic system for the synthesis of alkyl lactates in the presence of acidic ionic liquids. *Catalysts* **2020**, *10*, doi:10.3390/catal10010037.
10. Pereira, C.S.M.; Silva, V.M.T.M.; Rodrigues, A.E. Ethyl lactate as a solvent: Properties, applications and production processes—A review. *Green Chem.* **2011**, *13*, 2658–2671, doi:10.1039/c1gc15523g.
11. Kua, Y.L.; Gan, S.; Morris, A.; Ng, H.K. Ethyl lactate as a potential green solvent to extract hydrophilic (polar) and lipophilic (non-polar) phytonutrients simultaneously from fruit and vegetable by-products. *Sustain. Chem. Pharm.* **2016**, *4*, 21–31, doi:10.1016/j.scp.2016.07.003.
12. Kua, Y.L.; Gan, S.; Morris, A.; Ng, H.K. Liquid-Liquid Equilibrium Data for the Ternary Systems of Palm Oil + Ethyl Lactate + Phytonutrients (Carotenes and Tocols) at 303.15 K. *Int. J. Chem. Eng. Appl.* **2017**, *8*, 215–220, doi:10.18178/ijcea.2017.8.3.659.
13. Kua, Y.L.; Gan, S.; Morris, A.; Ng, H.K. Simultaneous Recovery of Carotenes and Tocols from Crude Palm Olein Using Ethyl Lactate and Ethanol. *J. Phys. Conf. Ser.* **2018**, *989*, doi:10.1088/1742-6596/989/1/012005.
14. Planer, S.; Jana, A.; Grela, K. Ethyl Lactate: A Green Solvent for Olefin Metathesis. *ChemSusChem* **2019**, *12*, 4655–4661, doi:10.1002/cssc.201901735.
15. Matsuda, H.; Inaba, K.; Sumida, H.; Kurihara, K.; Tochigi, K.; Ochi, K. Vapor-liquid equilibria of binary and ternary mixtures containing ethyl lactate and effect of ethyl lactate as entrainer. *Fluid Phase Equilib.* **2016**, *420*, 50–57, doi:10.1016/j.fluid.2015.12.029.
16. EPA Propyl L-Lactate. Available online: https://comptox.epa.gov/dashboard/dsstoxdb/results?search=DTXSID3042344#exposure. (accessed on 23 June 2020).
17. Woo, D.; Shin, J.; Sam, M.; Bae, W.; Kim, H. High-pressure phase behavior of propyl lactate and butyl lactate in supercritical carbon dioxide. *J. Chem. Thermodyn.* **2012**, *47*, 177–182, doi:10.1016/j.jct.2011.10.010.
18. Zheng, S.; Cheng, H.; Chen, L.; Qi, Z. Feasibility of bio-based lactate esters as extractant for biobutanol recovery: (Liquid + liquid) equilibria. *J. Chem. Thermodyn.* **2016**, *93*, 127–131, doi:10.1016/j.jct.2015.10.003.
19. Pereira, C.S.M.; Pinho, S.P.; Silva, V.M.T.M.; Rodrigues, A.E. Thermodynamic equilibrium and reaction kinetics for the esterification of lactic acid with ethanol catalyzed by acid ion-exchange resin. *Ind. Eng. Chem. Res.* **2008**, *47*, 1453–1463, doi:10.1021/ie071220p.
20. Stadler, B.M.; Wulf, C.; Werner, T.; Tin, S.; De Vries, J.G. Catalytic Approaches to Monomers for Polymers Based on Renewables. *ACS Catal.* **2019**, *9*, 8012–8067, doi:10.1021/acscatal.9b01665.
21. Solas, M.; Suárez-Pantiga, S.; Sanz, R. Ethyl lactate as a renewable carbonyl source for the synthesis of diynones. *Green Chem.* **2019**, *21*, 213–218, doi:10.1039/c8gc03275k.

22. Dusselier, M.; Van Wouwe, P.; Dewaele, A.; Makshina, E.; Sels, B.F. Lactic acid as a platform chemical in the biobased economy: The role of chemocatalysis. *Energy Environ. Sci.* **2013**, *6*, 1415–1442, doi:10.1039/c3ee00069a.
23. Bykowski, D.; Grala, A.; Sobota, P. Conversion of lactides into ethyl lactates and value-added products. *Tetrahedron Lett.* **2014**, *55*, 5286–5289, doi:10.1016/j.tetlet.2014.07.103.
24. Shuklov, I.A.; Dubrovina, N.V.; Kühlein, K.; Börner, A. Chemo-Catalyzed Pathways to Lactic Acid and Lactates. *Adv. Synth. Catal.* **2016**, *358*, 3910–3931, doi:10.1002/adsc.201600768.
25. Grala, A.; Ejfler, J.; Jerzykiewicz, L.B.; Sobota, P. Chemoselective alcoholysis of lactide mediated by a magnesium catalyst : An efficient route to alkyl lactyllactate. *Dalt. Trans.* **2011**, *40*, 4042–4044, doi:10.1039/c1dt10087d.
26. Maki-Arvela; Simakova, I.L.; Salmi, T.; Murzin, D.Y. Production of Lactic Acid/Lactates from Biomass and Their Catalytic Transformations to Commodities. *Chem. Rev.* **2014**, *114*, 1909–1971, doi:10.1021/cr400203v.
27. Vivian, A.; Fusaro, L.; Debecker, D.P.; Aprile, C. Mesoporous Methyl-Functionalized Sn-Silicates Generated by the Aerosol Process for the Sustainable Production of Ethyl Lactate. *ACS Sustain. Chem. Eng.* **2018**, *6*, 14095–14103, doi:10.1021/acssuschemeng.8b02623.
28. Cosate de Andrade, M.F.; Souza, P.M.S.; Cavalett, O.; Morales, A.R. Life Cycle Assessment of Poly(Lactic Acid) (PLA): Comparison Between Chemical Recycling, Mechanical Recycling and Composting. *J. Polym. Environ.* **2016**, *24*, 372–384, doi:10.1007/s10924-016-0787-2.
29. Song, X.; Zhang, X.; Wang, H.; Liu, F.; Yu, S.; Liu, S. Methanolysis of poly(lactic acid) (PLA) catalyzed by ionic liquids. *Polym. Degrad. Stab.* **2013**, *98*, 2760–2764, doi:10.1016/j.polymdegradstab.2013.10.012.
30. Petrus, R.; Bykowski, D.; Sobota, P. Solvothermal Alcoholysis Routes for Recycling Polylactide Waste as Lactic Acid Esters. *ACS Catal.* **2016**, *6*, 5222–5235, doi:10.1021/acscatal.6b01009.
31. Alberti, C.; Damps, N.; Meißner, R.R.R.; Enthaler, S. Depolymerization of End-of-Life Poly(lactide) via 4-Dimethylaminopyridine-Catalyzed Methanolysis. *ChemistrySelect* **2019**, *4*, 6845–6848, doi:10.1002/slct.201901316.
32. Alberti, C.; Damps, N.; Meißner, R.R.R.; Hofmann, M.; Rijono, D.; Enthaler, S. Selective Degradation of End-of-Life Poly (lactide) via Alkali-Metal-Halide Catalysis. *Adv. Sustain. Syst.* **2020**, *4*, 1900081–1900090, doi:10.1002/adsu.201900081.
33. Mckeown, P.; Roman-Ramírez, Luis, A.; Bates, S.; Wood, J. Zinc Complexes for PLA Formation and Chemical Recycling : Towards a Circular Economy. *ChemSusChem* **2019**, *12*, 5233–5238, doi:10.1002/cssc.201902755.
34. Román-Ramírez, Luis, A.; Mckeown, P.; Jones, M.D.; Wood, J. Poly(lactic acid) degradation into methyl lactate catalyzed by a well-defined Zn(II) complex. *ACS Catal.* **2019**, *9*, 409–416, doi:10.1021/acscatal.8b04863.
35. Madhavan Nampoothiri, K.; Nair, N.R.; John, R.P. An overview of the recent developments in polylactide (PLA) research. *Bioresour. Technol.* **2010**, *101*, 8493–8501, doi:10.1016/j.biortech.2010.05.092.
36. Kolstad, J.J.; Vink, E.T.H.; Wilde, B. De; Debeer, L. Assessment of anaerobic degradation of Ingeo polylactides under accelerated landfill conditions. *Polym. Degrad. Stab.* **2012**, *97*, 1131–1141, doi:10.1016/j.polymdegradstab.2012.04.003.
37. Shogren, R.; Wood, D.; Orts, W.; Glenn, G. Plant-based materials and transitioning to a circular economy. *Sustain. Prod. Consum.* **2019**, *19*, 194–215, doi:10.1016/j.spc.2019.04.007.
38. Volodymr, B.; Varvarin, A.; Svetlana, L.; Ya, G. Vapor-phase synthesis of lactide from ethyl lactate over TiO2/SiO2 catalyst. *Ukr. Chem. J.* **2019**, *85*, doi:10.33609/0041-6045.85.7.2019.31-37.
39. De Clercq, R.; Dusselier, M.; Makshina, E.; Sels, B.F. Catalytic Gas-Phase Production of Lactide from Renewable Alkyl Lactates. *Angew. Chemie Int. Ed.* **2018**, *57*, 3074–3078, doi:10.1002/anie.201711446.
40. De Clercq, R.; Dusselier, M.; Poleunis, C.; Debecker, D.P.; Giebeler, L.; Oswald, S.; Makshina, E.; Sels, B.F. Titania-Silica Catalysts for Lactide Production from Renewable Alkyl Lactates: Structure-Activity Relations. *ACS Catal.* **2018**, *8*, 8130–8139, doi:10.1021/acscatal.8b02216.
41. Upare, P.P.; Hwang, Y.K.; Chang, J.S.; Hwang, D.W. Synthesis of lactide from alkyl lactate via a prepolymer route. *Ind. Eng. Chem. Res.* **2012**, *51*, 4837–4842, doi:10.1021/ie202714n.
42. Egiazaryan, T.A.; Makarov, V.M.; Moskalev, M. V.; Razborov, D.A.; Fedushkin, I.L. Synthesis of lactide from alkyl lactates catalyzed by lanthanide salts. *Mendeleev Commun.* **2019**, *29*, 648–650, doi:10.1016/j.mencom.2019.11.014.

43. Payne, J.; Mckeown, P.; Mahon, M.F.; Emanuelsson, E.A.C.; Jones, M.D. Mono- and dimeric zinc(II) complexes for PLA production and degradation into methyl lactate—A chemical recycling method. *Polym. Chem.* **2020**, *11*, 2381–2389, doi:10.1039/d0py00192a.
44. Román-Ramírez, L.A.; McKeown, P.; Shah, C.; Abraham, J.; Jones, M.D.; Wood, J. Chemical Degradation of End-of-Life Poly(lactic acid) into Methyl Lactate by a Zn(II) Complex. *Ind. Eng. Chem. Res.* **2020**, doi:10.1021/acs.iecr.0c01122.
45. Román-Ramírez, L.A.; McKeown, P.; Jones, M.D.; Wood, J. Kinetics of Methyl Lactate Formation from the Transesterification of Polylactic Acid Catalyzed by Zn(II) Complexes. *ACS Omega* **2020**, *5*, 5556–5564, doi:10.1021/acsomega.0c00291.
46. Alaerts, L.; Augustinus, M.; Van Acker, K. Impact of bio-based plastics on current recycling of plastics. *Sustain.* **2018**, *10*, doi:10.3390/su10051487.
47. Cornell, D.D. Biopolymers in the existing postconsumer plastics recycling stream. *J. Polym. Environ.* **2007**, *15*, 295–299, doi:10.1007/s10924-007-0077-0.
48. McKeown, P.; McCormick, S.N.; Mahon, M.F.; Jones, M.D. Highly active Mg(ii) and Zn(ii) complexes for the ring opening polymerisation of lactide. *Polym. Chem.* **2018**, *9*, 5339–5347, doi:10.1039/c8py01369a.